Biol Cybern (2006) 94: 427–443
DOI 10.1007/s00422-006-0059-7

ORIGINAL PAPER

Biological Cybernetics

Aymar de Rugy · Robin Salesse · Olivier Oullier
Jean-Jacques Temprado

A neuro-mechanical model for interpersonal coordination

Received: 9 March 2005 / Accepted 1 February 2006 / Published online: 9 March 2006

Abstract The present study investigates the coordination between two people oscillating handheld pendulums, with a special emphasis on the influence of the mechanical properties of the effector systems involved. The first part of the study is an experiment in which eight pairs of participants are asked to coordinate the oscillation of their pendulum with the other participant's in an in-phase or antiphase fashion. Two types of pendulums, A and B, having different resonance frequencies (Freq A=0.98 Hz and Freq B=0.64 Hz), were used in different experimental combinations. Results confirm that the preferred frequencies produced by participants while manipulating each pendulum individually were close to the resonance frequencies of the pendulums. In their attempt to synchronize with one another, participants met at common frequencies that were influenced by the mechanical properties of the two pendulums involved. In agreement with previous studies, both the variability of the behavior and the shift in the intended relative phase were found to depend on the task-effector asymmetry, i.e., the difference between the mechanical properties of the effector systems involved. In the second part of the study, we propose a model to account for these results. The model consists of two cross-coupled neuro-mechanical units, each composed of a neural oscillator driving a wrist-pendulum system. Taken individually, each unit reproduced the natural tendency of the participants to freely oscillate a pendulum close to its resonance frequency. When cross-coupled through the vision of the pendulum of the other unit, the two units entrain each other and meet at a common frequency influenced by the mechanical properties of the two pendulums involved. The ability of the proposed model to address the other effects observed as a function of the different conditions of the pendulum and intended mode of coordination is discussed.

Keywords Rhythmic movements · Coordination dynamics · Coupling · Pendulum · Resonance frequency · Neural oscillator

A. de Rugy (✉)
Perception and Motor Systems Laboratory,
School of Human Movement Studies,
University of Queensland,
Room 424, Building 26, St Lucia,
QLD 4072, Australia
E-mail: aymar@hms.uq.edu.au
Tel.: +61-7-3365-6104
Fax: +61-7-3365-6877

A. de Rugy · R. Salesse · J.-J. Temprado
UMR Mouvement et Perception,
CNRS & Université de la Mediterranée,
Marseille, France

O. Oullier
Laboratoire de Neurobiologie Humaine (UMR 6149),
Université de Provence & CNRS, Marseille, France

1 Introduction

Recent studies have shown that the mere observation of the movement of another person's movement affects motor responses strongly enough to interfere with one's execution of a similar action, whether they move their own limbs (e.g., Kilner et al. 2003; O. Oullier, G.C. de Guzman, K.J. Jantzen, J. Lagarde and J.A.S. Kelso, submitted) or oscillate pendulums (Schmidt and O'Brien 1997). Moreover, when instructed to intentionally coordinate rhythmic movements, dyads of visually coupled participants can maintain stable interpersonal relative phase patterns over a wide range of movement frequencies and effector spatial orientations (Oullier et al. 2003; Schmidt et al. 1990, 1998; Temprado and Laurent 2004; Temprado et al. 2003). In the present study, we report an experiment and propose a model as to how interpersonal coordination of pendulum oscillations emerges from visual coupling and is influenced by the mechanical properties of the effector systems involved.

With the specific attempt to manipulate experimentally the mechanical properties of the effector system, Turvey and colleagues initially introduced an experimental protocol that involves participants oscillating pendulums with their wrist (Kugler and Turvey 1987; Turvey et al. 1986). When a single pendulum is freely oscillated, they show that participants

spontaneously established a frequency that is close to the resonance frequency of the pendulum. Since then, this capability of humans to tune the resonance frequency of a mechanical system has been reported in the context of vertical elbow oscillation with an external spring load by adults (Hatsopoulos and Warren 1996) as well as in babies placed on a bouncing support (Goldfield et al. 1993). Goodman et al. (2000) further revealed that oscillatory movements at resonance frequencies are more predictable and have a lower dimensionality than movements performed at other frequencies. In the context of pendulum oscillations, the attraction of the behavior toward the resonance frequency was revealed recently by Yu et al. (2003) in a continuation paradigm (Jantzen et al. 2004; Wing and Kristofferson 1973): participants had to first synchronize the oscillation of a pendulum on a periodic stimulus train and then continue their rhythmic response at the frequency of the stimulus after the stimulus had been turned off. When the frequency of the stimulus differed from the preferred frequency, a systematic drift toward the latter was observed in the continuation period.

Such influence of the mechanical properties of the effector system in rhythmic coordination has also been revealed in bimanual coordination, when one individual oscillates two pendulums simultaneously. In this context, a common frequency influenced by the resonance frequencies associated with each of the pendulums involved is typically observed (Kugler and Turvey 1987; Turvey et al. 1986). This common frequency has been accounted for by considering the resonance frequency of the compound system constituted by the two pendulums linked rigidly (e.g., Turvey et al. 1986). The mechanism underlying the production of this common frequency, however, remains to be explored further. Indeed, the mechanical coupling between the two hands may be expected to be rather weak. Recent evidence for a contralateral spread of excitability to the cortical representations of homologous muscle groups during rhythmic voluntary movements of a single limb, however, suggest that a direct neuro-muscular coupling is involved in the synchronization to a common frequency observed in bimanual coordination (Carson et al. 1999, 2004). For our case of interpersonal coordination (i.e., when two participants attempt to synchronize on each other's pendulum), however, neither the mechanical nor the neuromuscular coupling can operate, but only a visual coupling between the participants.

In the present contribution, we propose a neuro-mechanical model specifically designed to reproduce both the natural tendency to oscillate an individual pendulum at its resonance frequency and the emergence of an intermediate common frequency under the influence of the visual coupling. This was enabled by the conceptual distinction between the neural level and the mechanical-effector level. A similar distinction has been drawn recently by numerous authors to address various aspects of rhythmic coordination (e.g., Beek et al. 2002; Cattaert et al. 1999; de Rugy and Sternad 2003; de Rugy et al. 2003; Hatsopoulos 1996; Jirsa and Haken 1997; Peper et al. 2000, 2004b; Sternad et al. 1998; Taga 1995a,b, 1998; Williamson 1998, 2003). With respect to resonance tuning, this distinction was crucial in the design of a proprioceptive feedback that allowed a neural oscillator to be sensitive to, and tend toward, the resonance frequency of the effector system. Although close to the model proposed by Hatsopoulos (1996), the neuro-mechanical unit we propose presents a different influence of the proprioceptive feedback on the neural oscillator and incorporates an extra mechanism that consists of an adaptation of the time constant of the neural oscillator dynamics. These modifications proved to increase considerably the resonance tuning capabilities of the model and also to allow its development toward interpersonal coordination. These points will be addressed specifically in Sect. 3.1. The neuro-mechanical unit we propose also differs substantially from the one-layer model for resonance tuning developed by Bingham (1995), which consists of a simple linear damped mass-spring oscillator driven as a function of its own phase. A shortcoming of this model is that it oscillates necessarily at resonance frequency. The only way to produce oscillations over a range of different frequencies is therefore to modify the resonance frequency of the system. Although this could be done to a certain extent through modifications of the muscular stiffness (e.g., Latash 1992), this approach failed to account for the strong tendency to oscillate at a specific frequency associated with a given pendulum (e.g., Yu et al. 2003). Furthermore, it is hard to understand how such a mechanism could accommodate for frequencies that would require muscular stiffness to drop below its absolute minimum (i.e., zero) (see Peper et al. 2004a). In the context of the neuro-mechanical unit we propose, an external signal of arbitrary frequency can easily entrain the neural level, and thereby the whole system, independently of any modification of the mechanical properties of the effector system. The development of this model for interpersonal coordination consists of two neuro-mechanical units, one representing each participant, that are mutually coupled at the neural level through the vision of the oscillation of the other unit. In this model developed for interpersonal coordination, the common frequency is expected to emerge from both the entrainment property resulting from the mutual coupling between units and the natural tendency of each unit to oscillate at the resonance frequency associated with its effector system.

In order to test our model, an experiment was conducted involving pairs of participants to synchronize the oscillation of their pendulum with each other. Two different types of pendulum, having different mechanical properties, were used. The preferred frequencies associated with pendulums oscillated individually were assessed both at the beginning and at the end of the experiment. Because we are interested in the common frequency spontaneously established by participants when they attempt to synchronize on each other, no constraints were imposed on the frequency to produce in this coupling condition. A constraint on the intended phase of coordination, however, was included. Participants of each tested pairs had to synchronize either in-phase (i.e., a relative phase of 0° or 360° between angular displacements of pendulums) or antiphase (i.e., a relative phase of 180°) with each other. These conditions were designed to document further

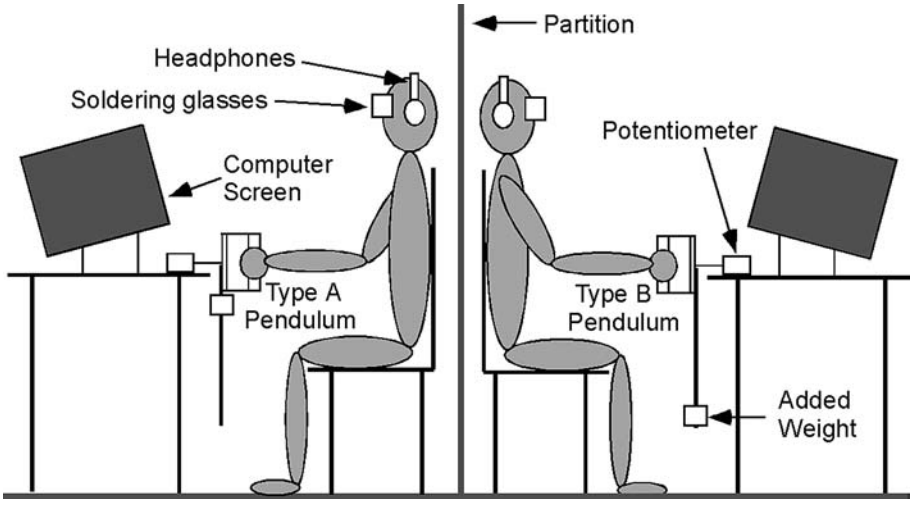

Fig. 1 Schematic representation of the experimental setup

the differential stability for these two patterns of interpersonal coordination (e.g., Amazeen et al. 1995; Oullier et al. 2003; Schmidt et al. 1998; Temprado and Laurent 2004). The ability of the proposed model to address this issue as well as other effects observed as a function of the different pendulum conditions will be developed in the Sect. 4.

2 Experiment

2.1 Method

2.1.1 Participants

Sixteen participants (13 males and 3 females) volunteered in this experiment. Participants were randomly divided into eight pairs. Their ages ranged from 24 to 37 years. All participants reported themselves to be right-handed with normal or corrected-to-normal vision. Participants were naive to the purpose of the experiment and filled a priori informed consent forms to participate in the experiment. The experiment received full approval from the local Ethics Committee.

2.1.2 Experimental setup and data acquisition

Participants were tested in pairs. Each participant comfortably sat on a chair in front of a computer screen. In order to control the visual exchange between them, vision of the other participant was prevented by a partition as illustrated in Fig. 1. The experiment was performed in the dark and participants wore soldering glasses. As a result, they could not see the movements of their own hand. This procedure also ensured that they could only see what was displayed on the screen in front of them. To suppress auditory information participants wore headphones through which a white noise was delivered binaurally.

Each participant grabbed a vertical dowel (17 cm length) with his/her right hand. The dowel was attached to a parallel bar whose center was fixed to a rotating horizontal shaft. Each shaft was equipped with a potentiometer in order to record angular displacement of the pendulums. An aluminum rod (50 cm) was fixed to the lower part of the parallel bar and received a lead weight (0.54 kg). This additional weight was either fixed at the top of the rod (Pendulum A, eigenfrequency=0.98 Hz, inertia=0.069 kg m^{-2}) or at the bottom (Pendulum B, eigenfrequency=0.64 Hz, inertia=0.379 kg m^{-2}). The total weight of both pendulums was 1.03 kg. Chairs and pendulum positions were adjusted so that participants grasped the middle of the dowel with their elbow flexed at approximately 120°, the long axis of their forearm being in line with the axis of rotation. In such posture, participants oscillated the pendulums by a pronation and supination movement of their forearm. Angular displacements of the pendulums were recorded at a sampling rate of 100 Hz.

The angular displacement of the pendulum manipulated by one subject was displayed online on the screen of the other participant. The effective angular displacements were displayed as linear horizontal displacements of a white dot (diameter 2 cm) on the screen. A scaling was applied so that the left or right extreme positions of the display (width 36 cm) corresponded to the maximal angular displacements allowed, −90° or +90°, respectively. The vertical position of the pendulum was the reference (0°) and was displayed in the middle of the screen. The refresh rate of each screen was 100 Hz.

2.1.3 Procedure and design

2.1.3.1 Control conditions Prior to the experiment, control conditions were performed to determine the participants' preferred oscillation frequency for each pendulum. Participants were instructed to swing the pendulum at their most comfortable frequency and amplitude. They performed a total of four trials (two per pendulum), the order of which was randomized. Each trial lasted for 40 s. At the beginning of each run, participants were displayed a 'GO' signal on their screen

for 1 s. This control procedure was repeated at the end of the experiment.

2.1.3.2 Experimental conditions The core of the experiment consisted of trials in which each participant was instructed to synchronize his/her pendulum oscillations with the oscillations of the other participant. Two intended modes of coordination were employed: *in-phase* (IN) and *antiphase* (ANTI). In the IN condition, participants were instructed to move the upper part of the handheld bar of the pendulums in the same direction as that of the motion displayed on the screen. Conversely, in the ANTI condition, they were instructed to oscillate the upper part of the handheld bar in a direction opposite to that of the motion displayed on the screen. Because it would be easy for participants to perform the ANTI condition by trying to synchronize the lower part (instead of the upper part) of the pendulum "in-phase" with the motion displayed on the screen, the instruction to consider the upper part of the handheld was repeated several times during the experiment.

In addition to these two intended modes of coordination, different combinations of pendulums manipulated by the two subjects were proposed. These pendulum conditions were AA (both participants manipulating a type A pendulum), AB (first participant of the pair with pendulum A and second with pendulum B), BA (first participant with pendulum B and second with pendulum A) and BB (both participants manipulated a type B pendulum).

Overall a total of eight experimental conditions were tested for each pairs resulting from fully crossing two Coordination modes (IN and ANTI) with four Pendulum combinations (AA, AB, BA and BB).

Similar to the control conditions, each experimental trial started with a 'GO' signal displayed for 1 s on the screen. This signal was followed by an initial time segment lasting 10 s during which nothing was presented on the screen and participants were instructed to produce, with a given pendulum (A or B), their preferred oscillatory movement. Subsequently the displacement of the pendulum of the other subject appeared on their screen for 40 s and participants were required to synchronize with it in a fashion (in- or antiphase) that was specified before each trial. Each experimental trial lasted 50 s.

IN and ANTI coordination mode conditions were blocked in two experimental sessions separated by a 15 min break. The order of these two sessions was counterbalanced, half of the pairs beginning with the IN session while the other half began with the ANTI session. Both sessions started with two practice trials with pendulum conditions determined randomly. This practice period was followed by a set of 12 trials, 3 trials per pendulum condition (AA, AB, BA and BB) presented in a randomized order. The added weight that defined the type of pendulum was moved to the center of the pendulum rod between each trial, before being repositioned to the appropriate location (up or down, for pendulum A or B, respectively). This was designed to prevent participants from inferring in advance the type of pendulum that was employed by the other participant (e.g., if the added weight was not moved between two trials, the participants would know that the same type of pendulum would be used on the next trials).

2.1.4 Data reduction and dependent measures

2.1.4.1 Time series reduction The time series of the pendulum's angular displacement for each trial was low-pass filtered using a zero-lag second-order Butterworth filter with a cutoff frequency at 8 Hz. This cutoff frequency was determined such that the autocorrelation function of the difference between the filtered and unfiltered data closely resembles white noise (Challis 1999). For each experimental trial, the first 10 s following the beginning of the presentation of visual feedback were discarded from analysis. It was expected that during this period the participants stabilized their movements in relation to the motion displayed on their screen. The remaining 30 s were analyzed to extract the pattern of coordination established.

2.1.4.2 Dependent variables Using a peak-picking algorithm the cycle-by-cycle frequency f (Hz) was calculated as the inverse of the mean period from the time series of each pendulum. The coefficient of variation of the frequency CVf was calculated, resulting from the standard deviation of the frequency being divided by the mean frequency. The means and coefficients of variation of the amplitude, A and CVA, respectively, were also computed. Amplitude was defined as $(\text{peak} - \text{valley})/2$. The primary dependent measure of coordination between the participants' oscillatory movements was the continuous relative phase determined in phase space, i.e., the space spanned between position and velocity for each oscillator. For both the considered pendulum θ_P and the target pendulum θ_T, the angular position was mean-adjusted by subtracting the average position. The angular velocity obtained by differentiation of angular position was normalized by dividing the velocity signal by the mean frequency. Next, the phase angles were computed for each sample of oscillatory movement as the arctangent of the position and velocity. Mean circular relative phase ψ was then determined using circular statistics (Fisher 1993). To this end, the cosine and sine of the difference between the phase angle for θ_P and θ_T were averaged separately, and ψ was obtained as the arctangent of their ratio (for more detail see Russell and Sternad 2001). In this calculation, θ_P movement was taken as the reference, meaning that positive values of ψ indicate that the considered pendulum is leading the target pendulum displayed on the screen. A measure of dispersion of circular relative phase, uniformity U, was calculated according to Fisher (1993). As this measure is bounded by 0 and 1 and is nonlinear with respect to the distribution around the mean relative phase angle, it is converted into a measure of dispersion SDψ that varies approximately linearly between 0 and infinity according to

$$\mathrm{SD}\psi = \left(-2\log_e U\right)^{1/2}.$$

As in the linearly computed standard deviation measure, high values of SDψ denote high variability, and low values indicate low variability.

Finally, for each of the experimental trial, the asymmetry (δ) was defined as the difference between the individual preferred frequency associated with the considered participant and pendulum ($\overline{f_{P,pref}}$) and the individual preferred frequency associated with the other participant manipulating the target pendulum displayed on the screen ($\overline{f_{T,pref}}$):

$$\delta = \overline{f_{P,pref}} - \overline{f_{T,pref}},$$

where $\overline{f_{P,pref}}$ and $\overline{f_{T,pref}}$ were obtained by averaging for each participant and pendulum the preferred frequency obtained from the control conditions.

2.1.4.3 Exclusion criteria A criterion for stability was set to remove trials in which frequency locking was not established and/or maintained for the analyzed period, as well as trials that presented a substantial drift in relative phase. This criterion corresponded to a dispersion of the relative phase (SDψ_{ci}) of 30°. A total of 14.8% of the trials presented a dispersion value higher than this criterion and were therefore discarded from analysis. The proportion of these trials that belonged to the antiphase mode of coordination (69%) was higher than for the in-phase mode of coordination (31%).

2.1.5 Statistical analyses

f, CVf, *A* and CVA obtained in the control trials were averaged and analyzed using a two-way repeated measures analysis of variance (16 participants) with two levels of Timing within the experiment (beginning and end) and two levels for the type of Pendulums (A and B).

Average frequencies and amplitudes obtained in the experimental trials were analyzed using a two-way repeated measures analysis of variance (eight pairs of participants) with two levels of intended modes of coordination (IN and ANTI) and four levels of Pendulum combination (AA, AB, BA and BB).

Quadratic regressions were performed on CVf, CVA and SDψ plotted against δ to test for the effect of task-effector asymmetry on the variability of the oscillatory behavior in the different experimental conditions. A U shape with a minimum close to zero asymmetry would denote that the variability of the behavior increases as a function of task-effector asymmetry. Paired *t* tests were performed to compare the variability of the behavior (CVf, CVA and SDψ) obtained in the two intended modes of coordination (IN and ANTI). Linear regressions were also performed on ψ against δ to test the effect of task-effector asymmetry on the pattern of coordination between participants of the same pair. Comparisons between slopes of these regressions were further performed using a *t* test. Linear and quadratic regressions were performed for IN and ANTI separately.

A significance level of $P<0.01$ was adopted for all statistical comparisons.

2.2 Results

2.2.1 Preferred oscillatory behavior (control conditions)

Preferred frequencies associated with oscillations of pendulum A (M=1.08 Hz, SD=0.091 Hz) were significantly higher than preferred frequencies of pendulum B (M=0.69 Hz, SD=0.071 Hz) [$F(1, 15)=548.67$, $P<0.001$]. These averaged preferred frequencies were slightly higher than the resonance frequency of the sole pendulums (0.98 and 0.64 Hz for pendulum A and B, respectively). No effects for the timing within the experiment and for the Pendulum × Timing interaction were obtained.

Preferred amplitudes were higher for pendulum B (M= 65.5°, SD=26.8°) than for pendulum A (M=51.6°, SD=16.9°) [$F(1, 15)=9.93$, $P<0.001$] and were higher at the end of the experiment (M=65.7°, SD=23.1°) than at the beginning (M=50.9°, SD=21.5°) [$F(1, 15)=15.16$, $P<0.001$]. No effect for the interaction between these factors was found.

As far as coefficients of variations are concerned, no effects for pendulum and timing of acquisition within the experiment were found on CVf or on CVA. On average, CVf was 1.71% and CVA was 5.59%.

2.2.2 Oscillatory behavior with visual exchange (experimental conditions)

2.2.2.1 Frequency and amplitudes of oscillation A significant effect of pendulum condition on frequencies at which participants synchronized was found [$F(3, 5) = 151.54$, $P<0.001$]. Figure 2 illustrates further that the average frequency adopted in pendulum condition AA (1.09 Hz) and BB

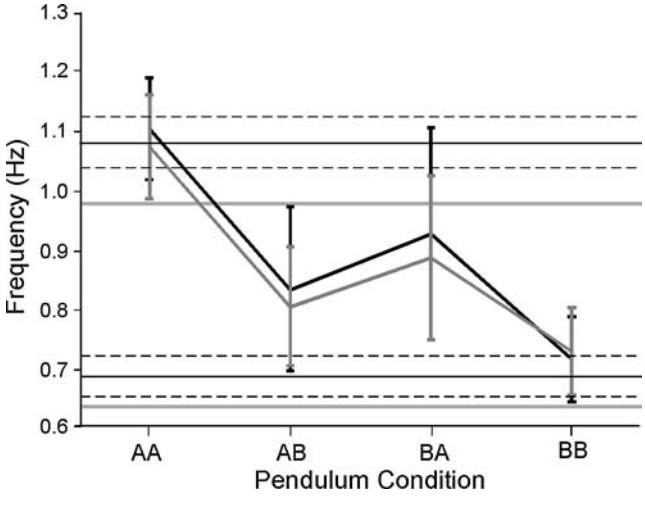

Fig. 2 Mean frequency obtained in coupling condition presented per coordination mode condition (IN in *black* and ANTI in *gray*) and per pendulum condition (AA, AB, BA and BB). *Gray lines* represent the resonance frequency associated with pendulums A (*top*) and B (*bottom*). *Dark lines* represent the averaged preferred frequencies of participants associated with pendulums A (*top*) and B (*bottom*) oscillated individually. *Dashed lines above and below the dark lines* represent the 95% confidence intervals around these preferred frequencies

(0.73 Hz) was close to the overall average preferred frequency for pendulum A (1.08 Hz) and B (0.69 Hz), respectively. Indeed the average frequency obtained for AA (for both IN and ANTI coordination mode conditions) was located within the 95% confidence intervals associated with average preferred frequency of pendulum A. As far as the other type of pendulum is concerned, the 95% confidence interval is exceeded by less than 0.01 Hz for ANTI only. On the other hand, the frequencies obtained for pendulum condition AB (0.82 Hz) and BA (0.91 Hz) are clearly situated in between the frequencies obtained for pendulum condition AA and BB. Figure 2 also illustrates that the intended mode of coordination appears to have little influence, which was confirmed by the lack of effect for coordination mode.

Mean amplitudes could not be distinguished between the experimental conditions, and the overall average of angular amplitudes is 52.9° (SD=16.6°).

Figure 3 shows CVf and CVA plotted against δ for each coordination mode, and Table 1 summarizes the coefficients of quadratic regressions performed on these data. For CVf, a U shape was obtained, which denotes higher variability in frequency performed with higher task-effector asymmetry. This effect occurred for both coordination modes and was confirmed by significant quadratic regressions and coefficients. Furthermore, Fig. 3 illustrates that the U shapes are slightly asymmetrical, with variability tending to be higher for positive values of δ than for negative ones. This effect was confirmed by significant linear coefficients (b on Table 1) and corresponds to higher variability of frequency when participants had to oscillate at a frequency lower than their preferred frequency (i.e., δ positive). Mean CVf obtained for conditions IN (2.72%) and ANTI (2.76%) could not be distinguished [$t(325)=0.27$, $P>0.05$]. As far as CVA is concerned, significant quadratic regressions were also obtained for both coordination mode. The linear trend was absent. Mean CVA obtained for conditions IN (6.20%) and ANTI (5.63%) could not be distinguished [$t(325)=1.94$, $P>0.05$].

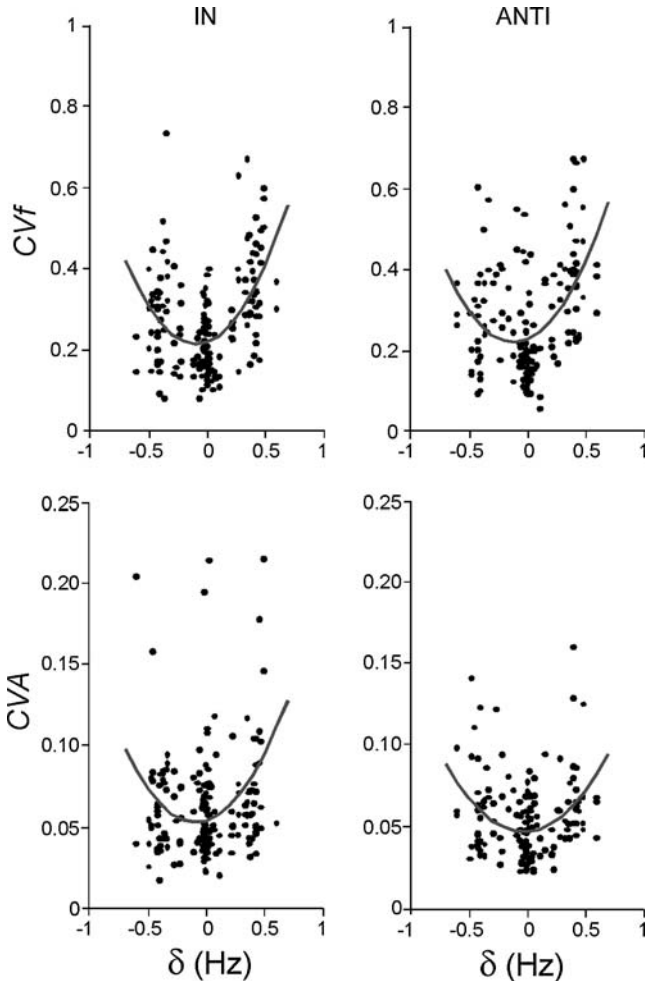

Fig. 3 CVf (*top*) and CVA (*bottom*) plotted against δ for the two intended modes of coordination, IN (*left*) and ANTI (*right*). *Gray lines* indicate quadratic regressions

2.2.2.2 Mean and variability of relative phase as a function of task-effector asymmetry Linear regressions performed on ψ against δ for both intended modes of coordination were significant. R^2 (slopes) of these regressions were 0.71 (35.0) and 0.66 (38.1) for IN and ANTI, respectively. Figure 4 (top) illustrates the linear relationship between ψ and δ. The relationship expresses a phase lead of the pendulum associated with the higher preferred period. Comparison between slopes of linear regressions in IN and ANTI did not reveal any significant differences [$t(325)=0.71$, $P>0.05$].

Quadratic regressions performed on SDψ against δ for both intended modes of coordination were significant. Figure 4 (bottom) illustrates the U shape obtained by plotting SDψ against δ. R^2 and coefficients of the regression are reported in Table 1. The U-shape corresponds to an increase in the variability of the relative phase as the task-effector asymmetry increasingly differs from 0. On the other hand, SDψ was on average lower for condition IN (0.189) than for condition ANTI (0.215) [$t(325)=3.06$, $P<0.01$], indicating a higher variability of the relative phase for the latter condition.

3 Model

3.1 Model description

The proposed model is composed of two coupled neuromechanical units, one per participant, each consisting of an effector level, modeled as a wrist-pendulum system, which interacts with the neural level, modeled as a neural oscillator (Fig. 5).

3.1.1 The effector level: wrist-pendulum systems

The effector level was modeled as two wrist-pendulum systems, i and j, described by

$$m_i l_{\mathrm{eq},i}^2 \ddot{\theta}_i + \gamma_i \dot{\theta}_i + m_i g l_{\mathrm{eq},i} \theta_i = k_i \left(\theta_{\mathrm{E},i} - \theta_i\right), \quad (1)$$

where θ_i is the angular displacement of the pendulum i, and the dots denote the first and second derivative. m_i, γ_i and

Table 1 Mean and standard error (SE) of the quadratic regression statistics for CVf, CVA and SDψ against asymmetry δ, obtained separately for each intended mode of coordination (IN and ANTI)

Variable	Condition	a		b		c		R^2	
		Mean	SE	Mean	SE	Mean	SE	Value	SE
CVf	IN	0.055*	0.009	0.010*	0.003	0.022*	0.001	0.237*	0.011
	ANTI	0.051*	0.010	0.011*	0.003	0.023*	0.001	0.209*	0.012
CVA	IN	0.121*	0.028	0.022	0.009	0.055*	0.004	0.125*	0.034
	ANTI	0.092*	0.020	0.004	0.007	0.048*	0.003	0.126*	0.024
SDψ	IN	0.374*	0.055	0.000	0.017	0.156*	0.007	0.215*	0.067
	ANTI	0.332*	0.062	−0.008	0.020	0.186*	0.008	0.160*	0.075

The coefficients a, b and c refer to the quadratic equation of the form $a\delta^2 + b\delta + c = 0$
Coefficients significantly different from zero are indicated by an asterisk (P<0.01)

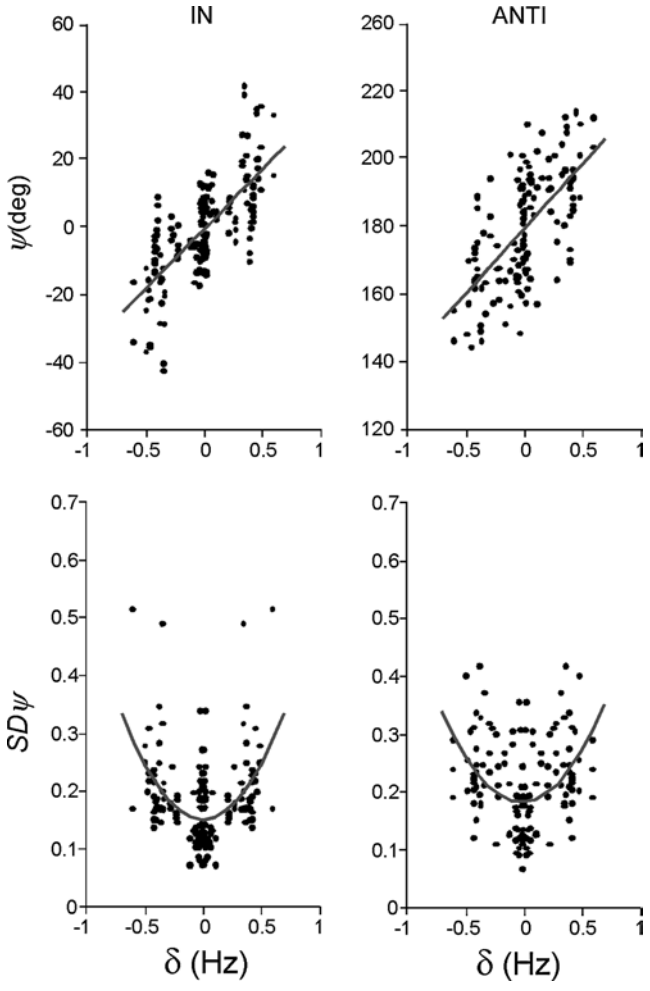

Fig. 4 ψ (*top*) and SDψ (*bottom*) plotted against δ for the two intended modes of coordination, IN (*left*) and ANTI (*right*). *Gray lines* indicate linear regressions on ψ and quadratic regressions on SDψ

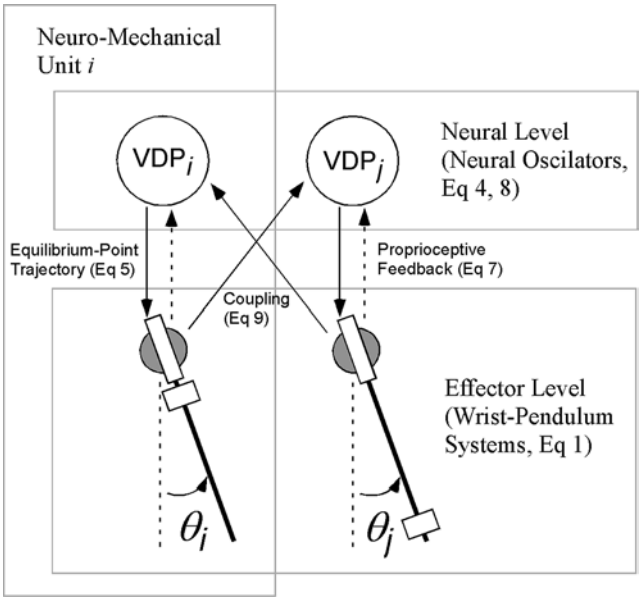

Fig. 5 Model description. Each participant is modeled as a neuro-mechanical unit (i or j), constituted of an effector level modeled as a wrist-pendulum system and a neural level modeled as a neural oscillator (VDP). Each neural oscillator drives its corresponding wrist-pendulum system by an equilibrium-point trajectory and receives in return a proprioceptive feedback. The two neuro-mechanical units are cross-coupled by the way of a signal from the other wrist-pendulum unit that inputs its neural oscillator. In this figure, the units i and j are represented with type A and B pendulums, respectively

$ml^2_{\mathrm{eq},i}$ are the mass, damping coefficient and the moment of inertia (I_i) associated with the wrist-pendulum systems i. $l_{\mathrm{eq},i}$ denotes the length of the equivalent point mass pendulum. The term $m_i g l_{\mathrm{eq},i}$ represents the gravitational stiffness of the pendulum. This term has been linearized for simplicity in the calculation of resonance frequency. Note that this simplification yields to a slight overestimation of the resonance frequency (e.g., Van Soest et al. 2004). The right side of Eq. (1) represents muscular torque developed as a function of the difference between the current angular position and an equilibrium angular position $\theta_{\mathrm{E},i}$ to be determined by the neural level. As such, k_i denotes muscular stiffness.

Assuming small values of damping, the resonance frequency $f_{\mathrm{P},i}$ (Hz) of the linearized pendulum i is

$$f_{\mathrm{P},i} = \frac{1}{2\pi}\sqrt{g/l_{\mathrm{eq},i}}. \tag{2}$$

As the experimental results show, however, the individually preferred frequencies f_{pref} are typically higher than the resonant frequencies of the mechanical pendulums ($f_{\mathrm{P},i}$).

This discrepancy had been attributed to the spring-like properties of muscle acting at the wrist (Kugler and Turvey 1987). Including this additional stiffness term [k_i on Eq. (1)] as well as damping [γ_i on Eq. (1)], the resonant frequency of the wrist-pendulum system $f_{\mathrm{WP},i}$ reads

$$f_{\mathrm{WP},i} = \frac{1}{2\pi}\sqrt{\left(g/l_{\mathrm{eq},i}\right) + \left(k_i/I_i\right) - \left(\gamma_i^2/4I_i^2\right)}. \quad (3)$$

3.1.2 The neural level: neural oscillators

The neural level was modeled as two Van der Pol (VDP) oscillators i and j

$$\begin{aligned} \tau_i \dot{u}_i &= w v + u_i - u_i^3/3 + h_{S,ij} S_{ij} + h_{P,i} P_i, \\ \tau_i \dot{v}_i &= -\varepsilon u_i, \end{aligned} \quad (4)$$

where u_i and v_i are state variables, τ_i a time constant that determines the frequency of the oscillation and w and ε parameters (Williamson 1999, adapted from Strogatz 1994). S_{ij} and P_i (and their gains, $h_{S,ij}$ and $h_{P,i}$) are the placeholders for the cross-coupling between units and for the proprioceptive feedback, respectively. While the VDP oscillator was originally designed for electronic circuits (Van der Pol 1926), it is the archetypal relaxation oscillator with two time scales and is therefore similar in character to the periodic bursting of neurons. Neural action potentials were explicitly modeled by Fitzhugh and Nagumo, but the VDP oscillator can be regarded a special case of their model that has been generally accepted as an appropriate model for neuronal firing (Fitzhugh 1957; Nagumo et al. 1962). In the present context, we therefore refer to the VDP as a neural oscillator representing the neural level.

3.1.3 Coupling and adaptive mechanisms

The coupling from the neural level to the effector level operated by the way of the equilibrium-point trajectory $\theta_{\mathrm{E},i}$, which is a function of the output u_i of the neural oscillator and drives the wrist-pendulum system [right side of Eq. (1)]. A noise term $\xi_{t,i}$ was added to u_i before the generation of $\theta_{\mathrm{E},i}$, in order to represent motor noise and to explore its effect on the variability of the simulated oscillatory behavior. $\theta_{\mathrm{E},i}$ is then given by:

$$\theta_{\mathrm{E},i} = h_{u,i}\left(u_i + \sqrt{Q}\xi_{t,i}\right), \quad (5)$$

where $h_{u,i}$ a gain, $\xi_{t,i}$ a zero-mean, unit variance, gaussian white noise and Q the variance of this added noise. An adaptation of the gain $h_{u,i}$ was designed to maintain the amplitude of oscillation in a range similar to that observed in the experiment. Maintaining the amplitude around a target amplitude A_t was obtained by a negative feedback loop operating on $h_{u,i}$ at every cycle n on the basis of the difference between A_t and the amplitude performed on the previous cycle A_{n-1}:

$$h_{u,i,n} = h_{u,i,n-1} + h_A(A_t - A_{n-1}), \quad (6)$$

where h_A is the gain of this adaptive feedback.

The coupling from the effector level to the neural level, which is required for resonance tuning, operated by way of a proprioceptive feedback P_i, which fed into the neural oscillator [Eq. (4)]. Williamson (1999) demonstrated that a VDP oscillator that drives a mechanical system drifts towards its resonance frequency when the VDP oscillator receives the velocity of the mechanical system as an input. Following Williamson (1999) we define P_i as:

$$P_i = \dot{\theta}_i. \quad (7)$$

The capability for resonance tuning of the system described so far, however, required a high gain of the proprioceptive feedback $h_{P,i}$ and remains limited to a relatively small range of frequencies. These shortcomings were withdrawn by an adaptation of the time constant τ_i of the neural oscillator, such that the frequency of the uncoupled neural oscillator follows the frequency that is currently produced. This adaptation is described by

$$r\dot{\tau}_i = -\tau_i + \tau_{c,i}, \quad (8)$$

where r is the adaptation rate of τ_i and $\tau_{c,i}$ is the time constant at which the frequency of the uncoupled neural oscillator equals the frequency that the neural oscillator currently produces ($f_{\mathrm{VDP},c,i}$). $\tau_{c,i}$ is determined on the basis of $f_{\mathrm{VDP},c,i}$ as explained in Sect. 3.2 [Eq. (10)]. Existing models based on neurophysiological studies that have demonstrated input-dependant modulation of the time constant of the membrane of neurons provide support for the mechanism described here (e.g., Bressloff 1995; Liu and Wang 2001).

As described so far, the neuro-mechanical unit described resembles the model for resonance tuning proposed by Hatsopoulos (1996), which also consists of a VDP oscillator that receives a proprioceptive feedback from a mechanical-effector system. In this model, the proprioceptive feedback affects directly the uncoupled frequency of the VDP. In the present model, however, the proprioceptive feedback intervenes at the level of the first state variable of the VDP oscillator [u_i in Eq. (4)], the uncoupled frequency of the VDP being modified indirectly by the adaptation of its time constant [Eq. (8)]. Those modifications offer several advantages. As already mentioned, the adaptation of the time constant increases considerably the range of resonance tuning capabilities of the system. Hatsopoulos (1996) reports resonance tuning for a range of 0.5–1.1 Hz and severe deterioration outside this range (cf. Fig. 3 in his article). The model proposed in this section has been successfully tested for resonance tuning in a range of 0.2–10 Hz (with parameter values described as in Sect. 3.2, except for the mechanical properties of the wrist-pendulum system that were modified to provide the given range of resonance frequency). Furthermore, the placeholder we used (following Williamson 1999) for the modulation of the dynamics of the VDP oscillator offers the advantage that it not only allows for resonance tuning under the influence of a proprioceptive feedback, but also for entrainment onto external signals. This feature, which is not shared by the model proposed by Hatsopoulos (1996), is indeed crucial for the coupling of two neuro-mechanical units to model interpersonal coordination (cf. next paragraph). As an additional

feature specific to the proposed model, the capacity to entrain on external signals together with the adaptation of the uncoupled frequency of the neural oscillator allows to simulate/reproduce results obtained in a continuation paradigm. Indeed, when participants were required to perpetuate a rhythm that was first imposed by an external signal and then removed, a slow drift toward the resonance frequency associated with the pendulum was observed. Importantly, this slow drift started from the frequency initially imposed, and no abrupt shift was observed at the moment of the removal of the external signal (Yu et al. 2003; H. Yu, A. de Rugy and D. Sternad, under revision). In the proposed neuro-mechanical model, if the neural oscillator had maintained its uncoupled frequency at a constant value different from the imposed frequency, the performed frequency would shift abruptly to this uncoupled frequency as soon as the external signal is removed (rather than drifting gradually toward the resonant frequency). With the time constant adaptation, however, the model is capable of reproducing the results obtained in a continuation paradigm, as shown by the adaptation of the model presented by Yu et al. (under revision).

Now that our neuro-mechanical units i and j are ready to tune the resonant frequency of the wrist-pendulum systems, it remains to couple them together. As mentioned above, the VDP oscillator can easily entrain and lock in phase with a rhythmic signal entered as S_{ij} in [Eq. (4)]. We also know from mechanics that driving a pendulum system at resonance frequency implies a 90° lag of the pendulum motion with respect to its driver. In-phase tracking of a sinusoid at resonance could therefore be achieved by entering the velocity of the sinusoid as an input to the neural oscillator: if the driver locks in-phase with the velocity of the sinusoid to track, the 90° lag of the pendulum motion with respect to the driver would be exactly compensated by the 90° lead of the velocity of the sinusoid with respect to the sinusoid itself. Furthermore, as the lead of the driver with respect to the pendulum increases and decreases when its frequency is, respectively, higher and lower than the resonance frequency of the mechanical system, phase lag or lead should occur at frequency that differs from the resonance frequency. This feature has the potential to reproduce the phase shift observed as a function of the effector asymmetry in the experiment (a similar logic is presented in Peper et al. 2004a,b, together with some of its limitations). Following this idea, each neural oscillator receives as an input the velocity signal of the angular motion of the pendulum of the other participant (i.e., neuro-mechanical unit):

$$S_{ij} = \dot{\theta}_j. \tag{9}$$

3.2 Parameterization

The mechanical characteristics of the simulated pendulums were set to correspond to that of the pendulums used in the experiment. The mechanical characteristics of the hand were further included by modeling the hand as a sphere of radius 0.05 m and mass 0.42 kg, corresponding to 0.6% of the total mass (70 kg) of an averaged participant (Dempster 1955). The resulting characteristics of the compound pendulum including the hand were m_{HA}=m_{HB}=1.45 kg; I_{HA}=0.100 kgm^2 and I_{HB}=0.534 kgm^2, $l_{eq,HA}$=0.262 m and $l_{eq,HB}$=0.609 m.

The damping ratio [i.e., the ratio between the damping coefficient (γ) and the critical damping] was set to 0.2. Since the critical damping is specific to each pendulum, the damping coefficients were different for pendulums A and B: γ_A=0.28 Nm rad^{-1} s^{-1} and γ_B=0.92 Nm rad^{-1} s^{-1}. Stiffness was set to k_A=k_B=1.2 Nm rad^{-1}. Damping and stiffness coefficients were determined such that the resonance frequency of the simulated wrist-pendulum system approximates the averaged preferred frequency produced by participants in the experiment.

Given these parameters, the resonance frequency of the wrist-pendulum system simulated with pendulums A and B are shown in Fig. 6, together with the averaged preferred frequency produced by participants in the experiment. This figure revealed that $f_{WP,A}$ and $f_{WP,B}$ gave reasonable approximation of the preferred frequencies obtained in the experiment. The figure also displays predictions from the compound pendulum constituted by pendulums A and B rigidly coupled, as well as frequencies spontaneously achieved by the neuro-mechanical model under different pendulum conditions. These predictions and simulation results will be explained in Sect. 3.3.

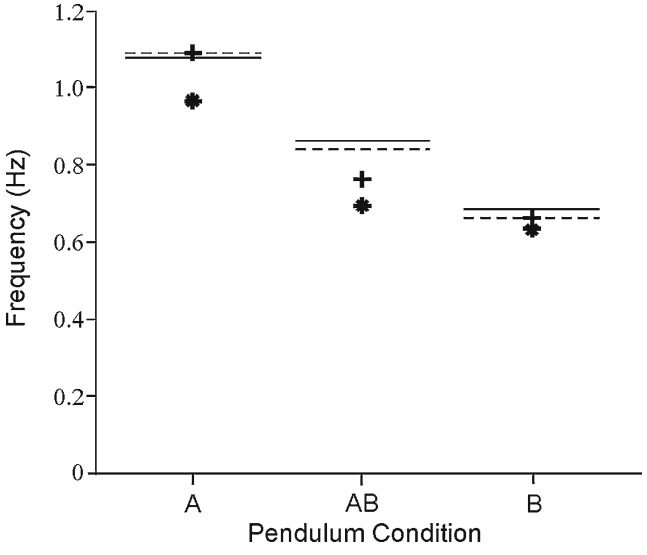

Fig. 6 Resonance frequencies of the modeled pendulum and wrist-pendulum systems together with the preferred frequencies spontaneously reached by participants and by simulation. *Stars* and *crosses* correspond to the resonance frequencies of the pendulum [Eq. (2)] and the wrist-pendulum systems [Eq. (3)], respectively. For condition AB, these resonance frequencies were calculated using the compound pendulum constituted by the rigidly linked pendulums A and B (see text for details). *Solid lines* correspond to the average preferred frequency spontaneously produced by participants, and *dashed lines* correspond to the frequency spontaneously established by simulation run using the neuro-mechanical model. For A and B, these lines correspond to frequencies established with pendulums A and B oscillated individually. For condition AB, both frequencies obtained and simulated in pendulum conditions AB and BA were averaged

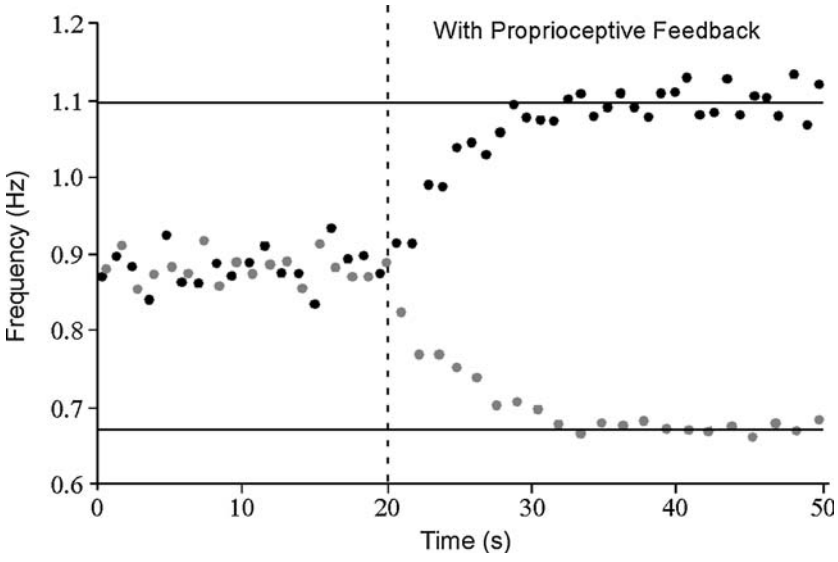

Fig. 7 Time series of the frequency obtained in a simulation of pendulums A and B oscillated individually without and with the operation of the proprioceptive feedback. *Dark and gray dots* represent frequencies of the pendulums A and B, respectively. The *vertical dashed line* indicates the initiation of the proprioceptive feedback. The *solid lines* represent the resonance frequencies of the wrist-pendulum systems. Without proprioceptive feedback, the pendulums oscillate at a frequency that depends on the initial parameter setting for the neural oscillator (similar for pendulums A and B in those simulations). When the proprioceptive feedback operates, both pendulums drift toward, and stabilize on, the resonance frequency associated with their respective wrist-pendulum system

The parameters of the VDP oscillator were set to ε=0.1 and w=0.817. As such, the VDP oscillator is strongly nonlinear, which proved to enhance the resonance tuning properties of the modeled system. With this parameterization and a time constant τ=0.03 s, the frequency of the uncoupled VDP oscillator is 1 Hz. Furthermore, the frequency of the uncoupled VDP oscillator is a linear function of the inverse of its time constant. The time constant $\tau_{c,i}$ at which the frequency of the uncoupled VDP equals the frequency that the VDP oscillator currently produces ($f_{\mathrm{VDP},c,i}$) is therefore given by

$$\tau_{c,i} = \frac{0.03}{f_{\mathrm{VDP},c,i}}. \tag{10}$$

The rate of the adaptation of the time constant τ_i based on $\tau_{c,i}$ [Eq. (8)] was r=0.5.

The gains on the inputs to the neural oscillators (i.e., the proprioceptive feedback P_i and the external signal S_{ij}) were set to $h_{P,i}$=0.02 and $h_{S,ij}$=0.05. These gains were sufficient to allow resonance tuning when the neuro-mechanical systems are uncoupled (i.e., $h_{S,ij}$=0), and permit frequency locking when they are coupled. Simulation of the antiphase intended pattern of coordination was simply achieved by changing the sign of $h_{S,ij}$, i.e., $h_{S,ij}$=−0.05.

The gain of the amplitude adaptation feedback loop was set to h_A=0.2, and the target amplitude was set to the averaged amplitude produced by participants, A_t=52°.

The variance of the white noise process [Eq. (5)] was set such that the variability in amplitude and frequency of the simulated oscillation matched on average those obtained in the experiment. Q=0.0225.

For all simulations the differential equations were numerically integrated using the Euler method of integration with a time step of 0.0025 s. Initial conditions were arbitrarily determined within the range of operation of the system.

3.3 Simulations

The first important aspect of the model is its capability for resonance tuning. Figure 7 confirms this feature by presenting on the same graph the time series of the frequency obtained in a simulation of pendulums A and B oscillated individually without and with the operation of the proprioceptive feedback. Without proprioceptive feedback, the pendulums oscillate at a frequency that depends on the initial parameter setting for the neural oscillator (similar for pendulums A and B in those simulations). When the proprioceptive feedback operates, however, both pendulums drift toward, and stabilize on, the resonance frequency associated with their respective wrist-pendulum system.

Figure 8a presents a simulation that mimics the experimental protocol with pendulums A and B, respectively, attributed to units i and j. This figure displays the time series of the frequency during 50 s, while the neuro-mechanical units are uncoupled for the first 10 s (S_{ij}=S_{ji}=0), and coupled for the remaining 40 s ($S_{ij} = \dot{\theta}_j$, $S_{ji} = \dot{\theta}_i$). The first 10 s uncoupled displayed began once the system had stabilized spontaneously on the resonance frequencies associated with its effector systems. Once the coupling operates, both systems quickly drift toward each other and lock at a common frequency that is between the resonance frequencies involved. This locking on a common intermediate frequency results from the balance of competition and cooperation between both neuro-mechanical units: each unit tends to drift toward

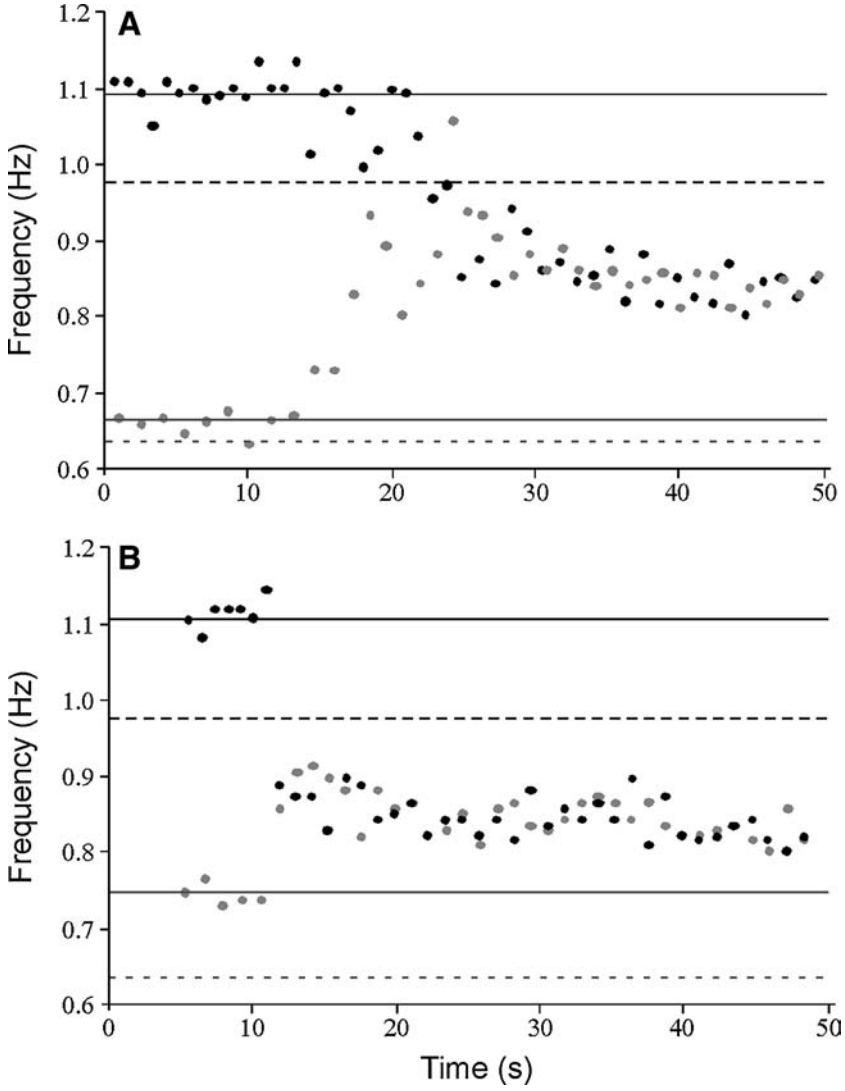

Fig. 8 Time series of the frequency obtained in a simulated (**a**) and representative (**b**) trials obtained in pendulum condition AB. *Dark and gray dots* represent frequencies of the pendulums A and B, respectively. The first 10 s were performed without coupling, while a coupling operates in the remaining 40 s. For the simulated data, the *solid lines* represent the resonance frequencies of the wrist-pendulum systems. For the trial from the experiment, the *solid lines* represent the preferred frequencies associated with the concerned participant and the pendulum used. In both panels, the *dashed lines* represent the resonance frequencies associated with the pendulums only. *Dark and gray lines* correspond to those frequencies associated with pendulums A and B, respectively

the resonance frequency associated with its effector system under the influence of the proprioceptive feedback, while at the same time the units tend to synchronize on each other under the influence of the visual coupling that inputs their respective neural level.

To provide a comparison with the behavior observed in the experiment, Fig. 8b displays an equivalent plot for a representative trial. Although the frequency locking takes longer to be established in the simulation than in the displayed example from the experiment, a similar intermediate frequency was achieved in both cases.

As an alternative justification for the common frequency spontaneously established by the system, Kugler and Turvey (1987) proposed that this frequency corresponds to the resonance frequency of the compound system, constituted by the two pendulums rigidly coupled. To provide new insight into this proposition, we determined the resonance frequency of the compound system constituted by pendulums A and B linked rigidly. According to Huygens's law, the equivalent length of the compound pendulum is

$$l_{\mathrm{eq,AB}} = \frac{m_{\mathrm{A}} l_{\mathrm{eq,A}}^2 + m_{\mathrm{B}} l_{\mathrm{eq,B}}^2}{m_{\mathrm{A}} l_{\mathrm{eq,A}} + m_{\mathrm{B}} l_{\mathrm{eq,B}}}. \tag{11}$$

To include the mechanical properties of the hand, $l_{\mathrm{eq,HAB}}$ was further calculated using Eq. (11) with $l_{\mathrm{eq,HA}}$, $l_{\mathrm{eq,HB}}$, m_{HA} and m_{HB}. The resonance frequency of the compound pendulums $f_{\mathrm{P,HAB}}$ was then calculated using $l_{\mathrm{eq,HAB}}$ in Eq. (2). As for the case of a pendulum oscillated individually, however, a preferred frequency higher than $f_{\mathrm{P,HAB}}$ could be justified by additional stiffness terms associated with the wrist-pendulum

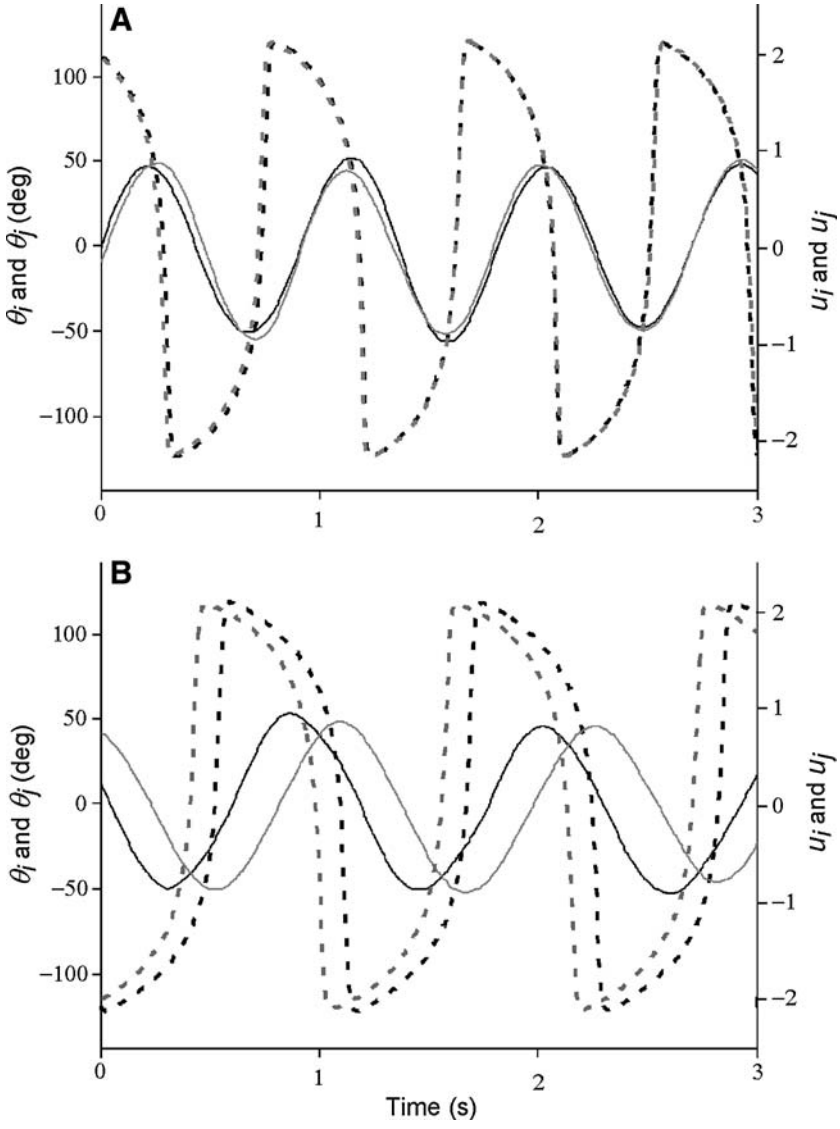

Fig. 9 Outputs of the neural oscillators (*dotted lines*) and pendulum angular displacements for simulation run with pendulum conditions AA (**a**) and AB (**b**). *Dark lines* represent unit *i* and *gray lines* unit *j*. In **b**, pendulum A is attributed to unit *i* (*dark*) and pendulum B is attributed to unit *j* (*gray*)

systems. To account for this, both the stiffness and damping of the compound system were set according to $k_{AB} = k_A + k_B$ and $\gamma_{AB} = \gamma_A + \gamma_B$, in order to calculate the resonant frequency of the compound wrist-pendulum system. The inertia of the compound system was then calculated using $m_{HAB} = m_{HA} + m_{HB}$ ($I_{HAB} = m_{HAB} l^2_{eq,HAB}$). Equation (3) was finally used with these parameters to calculate $f_{WP,HAB}$. Results of these calculations are displayed in Fig. 6, under the AB label. This figure show that these resonance frequencies for the rigidly linked compound system AB, if they are situated between the resonance frequency associated with pendulums A and B, remain noticeably closer to the second one (B). The high inertia associated with pendulum B is responsible for this feature. This prediction from the rigidly linked compound system, however, is not supported by the experimental results. Instead, the frequency established by participants in pendulum conditions AB and BA (solid line in Fig. 6) is approximately in the middle of the preferred frequencies associated with pendulums A and B. The model of coupled neuro-mechanical systems we propose, however, provides a good approximation of this feature (dashed line in Fig. 6).

To illustrate the relation between the neural level and the effector level, as well as the effect of the effector asymmetry on the relative phase between the pendulums, Fig. 9 shows the outputs of the neural oscillators and the motion of the pendulum for simulations run with pendulum conditions AA (Fig. 9a) and AB (Fig. 9b). For the case AA, both pendulums are in phase, which is also true for the output of the neural oscillators that drive their motions. Since the common

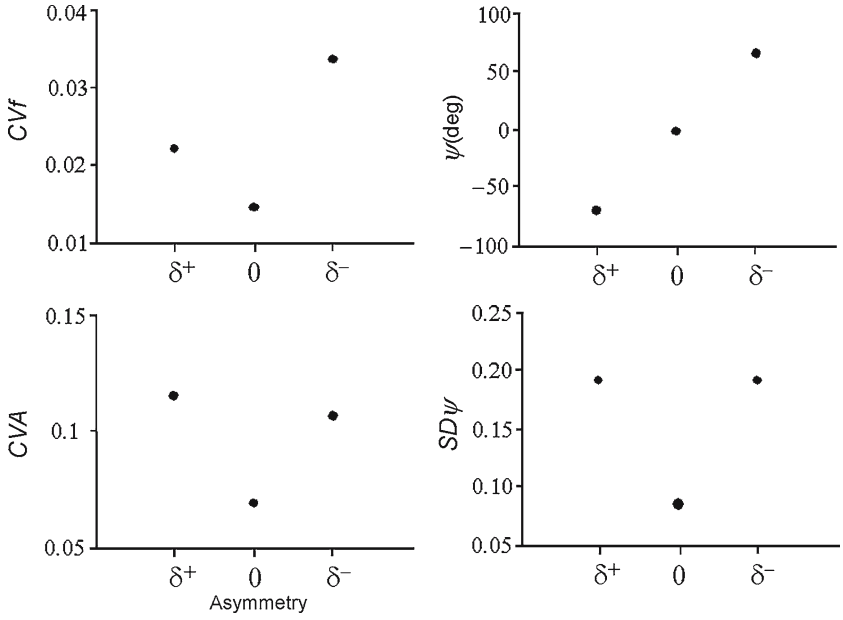

Fig. 10 Simulated results obtained for CVf, CVA, ψ and SDψ, plotted against the effector asymmetry δ. δ=0 corresponds to both simulations run with pendulums AA and BB. For CVA, CVf, δ^+ correspond to pendulum A in a AB (or equivalently BA) condition and, conversely, negative δ^- corresponds to pendulum B in AB or BA conditions

frequency established in this condition corresponds to the resonance frequency associated with the wrist-pendulum systems involved, the output of the neural oscillators lag the pendulum motions by approximately 90°. For AB, the pendulum A is clearly leading pendulum B in time. As we already reported, the common frequency established in this case is between the resonance frequencies associated with the neuro-mechanical units involved. Therefore, the pendulums A and B are oscillated at frequencies lower and higher than the resonance frequency associated their respective unit. This explains why the relation between the output of the neural oscillator and the pendulum motion is lower than 90° for pendulum A and higher than 90° for pendulum B. Since each neural oscillator receives the velocity signal from the pendulum of the other unit as input and tends to synchronize in phase with it, a relation opposite to the relation between pendulum motions exists between the outputs of the neural oscillators: the neural oscillator of the unit B leads the neural oscillator of the unit A.

In order to compare quantitatively the simulation from the neuro-mechanical model with the data from the experiment, a set of simulations were run for every pendulum condition, AA, AB, BA and BB, and the simulated data were analyzed in a similar way as the experimental data. To assess the effect of noise on a sufficiently large sample, simulations were run for 10 min without coupling, followed by 10 min with coupling between neuro-mechanical units. Simulations of the experimental condition ANTI were also conducted by inverting the sign of the velocity coupling between the neuro-mechanical units. Since no noticeable differences were found on results simulated for condition IN or ANTI, only simulations for the former are presented.

Figure 10 shows the simulated results obtained for CVf, CVA, SDψ and ψ, plotted against the effector asymmetry δ. As for the results from the experiment, simulated behavior is more variable as δ differs from zero. This is true for CVf, CVA and SDψ. The slightly asymmetrical effect of δ on CVf observed in the experiment is also reproduced in the simulated results, with higher variability of frequency for the neuro-mechanical system that oscillated at a common frequency lower than its own resonance frequency (i.e., for positive δ). Also in agreement with the experimental results is the more symmetrical pattern obtained for CVA. As far as the relative phase is concerned, the pendulums were in phase for δ=0, and a phase lead (lag) of the pendulum associated with the higher (lower) resonance frequency is produced. Although this effect is qualitatively similar to the effect observed in the experiment, its magnitude is noticeably higher for the simulated results.

4 Discussion

The goal of the present study was to develop, in conjunction with experimental data, a neuro-mechanical model for interpersonal coordination with a special emphasis on the influence of the mechanical properties of the effector systems on the common frequency established by participants when they attempt to synchronize the oscillation of their handheld pendulum with each other. The visual coupling between two neuro-mechanical units, individually capable of resonance tuning, was developed to account for this particular common frequency. The experiment was also designed to test for other effects that would be a function of the task-effector

asymmetry (i.e., the difference between the resonance frequency associated with the pendulums involved) and the intended mode of coordination (in-phase and antiphase). Experimental results revealed that the preferred frequencies produced by participants while manipulating each pendulum individually were slightly higher than the resonance frequencies of the pendulums. In their attempt to synchronize with one another, participants met at common frequencies that were situated between the preferred frequencies associated with the pendulums involved. Both the variability of the behavior and a shift in the intended relative phase were found to increase with the task-effector asymmetry. Only the variability of the relative phase was found higher for the antiphase mode of coordination than for the in-phase one. We will now discuss these results in relation to the literature and to the neuro-mechanical model we proposed.

The tendency for entrainment between oscillatory movements in living creatures has been reported by Von Holst (1973) in studies on the movement of fish fins. Based on his observation, Von Holst formulated two principles, i.e., the *maintenance tendency*, which refers to the tendency for each fin to oscillate at a frequency specific to it when oscillated individually, and the *magnet effect*, which refers to the tendency for entrainment to a common frequency between two fins oscillated simultaneously. In the context of handheld pendulum oscillation in humans, the first principle has been understood in terms of the resonance frequency of the wrist-pendulum system (Kugler and Turvey 1987). The results of the present experiment are consistent with this interpretation, since the participants reliably produced a preferred frequency that is close to the resonance frequency of the pendulums used, the small differences between these frequencies being easily accounted for by muscular stiffness acting at the level of the wrist. Furthermore, the resonance tuning property of the proposed neuro-mechanical unit provides an instantiation of a plausible mechanism responsible for the attraction of the behavior toward this particular frequency (e.g., Goldfield et al. 1993; Hatsopoulos and Warren 1996; Yu et al. 2003, under revision).

As far as the second principle is concerned, the entrainment to a particular common frequency when oscillated in combination has also been observed in the present experiment. From the many experiments conducted on handheld pendulums, either on bimanual or on interpersonal coordination, this particular common frequency has paradoxically received only little attention. Either the frequency of oscillation was imposed by a metronome (e.g., Treffner and Turvey 1995, 1996; Schmidt et al. 1998), or the common frequency established was not analyzed explicitly in relation to the mechanical properties of the pendulums involved (e.g., Schmidt et al. 1991; Schmidt and Turvey 1994). In other cases, the theoretical common frequency derived from the assumption of rigidly linked pendulums (Turvey et al. 1986) was calculated from the sole mechanical characteristics of the pendulums involved, in order to set the frequency to be imposed by a metronome in the experiments (e.g., Sternad et al. 1992, 1995; Collins et al. 1996; Amazeen et al. 1995). All the remaining studies which explored the common frequency actually established in a spontaneous fashion by participants have interpreted their results to be consistent with the rigidly linked pendulums idea (Turvey et al. 1986; Bingham et al. 1991; Schmidt et al. 1993; Sternad et al. 1996). In the present study, we further tested this hypothesis. Indeed, the mechanical properties of the pendulums used in the present experiment would predict, along with the rigidly linked hypothesis, the common frequency to be closer to the slower pendulum (B) when different pendulums were used (pendulum conditions AB and BA). The results, however, are not consistent with this hypothesis: the common frequency established by participants was more evenly situated between the resonance frequencies associated with individual pendulums (see Fig. 7). Alternatively, the particular common frequency found in the experiment has been successfully reproduced by simulation conducted with the proposed model. In this model, the common frequency emerges from the competition and cooperation between the two coupled neuro-mechanical units: each unit tends to drift toward the resonance frequency associated with its effector system under the influence of the proprioceptive feedback, while at the same time the units tend to entrain each other under the influence of the visual coupling that inputs their respective neural oscillators at the neural level. As such, this model provides a biologically plausible implementation of the mechanism underlying both the maintenance tendency and the magnet effect introduced by Vom Holst (1973), in the context of visually coupled oscillatory behavior.

The distinction between the neural and the mechanical levels that characterize our model further allows to address the nature of effects observed as a function of the effector asymmetry. The variability of the behavior that was found to increase as a function of the asymmetry in the experiment was reproduced by the model. Since the mechanical properties of the pendulums was the only parameter changed in order to simulate the different pendulum conditions, this increase of variability can be attributed to the influence of the mechanical properties of the effector system driven away from its resonance frequency.

The shift in the relative phase observed as a function of the asymmetry in the experiment constitutes another important effect that was qualitatively reproduced by the proposed model. As for the variability effects, this shift can be attributed to the influence of the mechanical properties of the effector system since only these properties were changed to simulate the different pendulum conditions. The shifts obtained in the simulation, however, are much higher than the ones observed in the experiment. This discrepancy might reflect the operation of an error-correction mechanism. Indeed, Russell and Sternad (2001) did not find any shift in relative phase as a function of the asymmetry when a cursor representing the pendulum was simultaneously displayed on a screen with a sinusoidal motion to track with the pendulum. In this situation, an error-correction mechanism could have operated in an efficient way on the basis of the visually available difference between the pendulum angular position and

the sinusoidal signal to track. When the cursor representing the pendulum motion was removed from the screen, however, a small phase shift reappeared (D.M. Russell, A. de Rugy and D. Sternad submitted). This phase shift is then likely to reflect a lower efficiency of the error-correction mechanism based on a less directly perceivable error signal. Another possibility is that participants adjusted their level of muscular stiffness in relation to the frequency they produced. In this context, Latash (1992) reported joint stiffness to increase or decrease as the frequency of motion increase or decrease, such that the resonance frequency of the effector system drift toward (but not enough to reach) the frequency produced. If a similar mechanism had occurred in our experiment, the real asymmetry operating would then be lower than the asymmetry considered in the simulation and would result in a lower phase shift. These two plausible explanations for the lower phase shift observed in experimental data, i.e., an error-correction mechanism and a modulation of stiffness, need to be further investigated and might be incorporated in the future development of the proposed model.

The present experiment also involved two conditions of intended relative phase for the synchronization, i.e., in-phase and antiphase, which are the two predominant patterns of coordination initially found in the context of bimanual movement (Yamanishi et al. 1980; Kelso 1981). Many studies on bimanual coordination had further revealed the higher stability associated with the in-phase pattern of coordination (e.g., Turvey et al. 1986; Schmidt et al. 1993; Sternad et al. 1996). Although Amazeen et al. (1995) and Temprado and Laurent (2004) found the variability of the behavior to be higher in antiphase than in in-phase for the case of interpersonal coordination, this effect seems to be less prominent than for bimanual coordination. Schmidt et al. (1998) provide the sole study that incorporates both in-phase and antiphase intended pattern of coordination in both the bimanual and the interpersonal case. While the effect was clear for the bimanual case, they failed to obtain a significant effect for the interpersonal case. In the present experiment, the effect was significant, indicating a higher stability for the in-phase than for the antiphase pattern of coordination. Another important effect obtained as a function of the coordination mode concerns the drift in the relative phase that occurs as a function of the effector asymmetry. This drift has indeed been typically observed to be higher for the antiphase than for the in-phase pattern of coordination, and this both for the case of bimanual (e.g., Schmidt et al. 1998; Sternad et al. 1996; Treffner and Turvey 1995) and interpersonal coordination (e.g., Schmidt et al. 1998). In the present experiment, however, this effect has not been observed. It is nevertheless important to note that in our experimental protocol, the in-phase and antiphase patterns of coordination were arbitrarily defined: participants had to move the upper part of the handheld in the same (in-phase) or opposite (antiphase) direction to that of the motion displayed on the screen (cf. Sect. 2.1). Although this instruction was repeated several times, participants could have switched their mode of coordination by considering the lower part of the handheld. In such a context of arbitrarily defined modes of coordination, Wimmers et al. (1992) also failed to observe mode-related changes in the behavior. The absence of effect might therefore result from the arbitrariness of the definition rather than indicating similar dynamics for the two modes of coordination.

At its stage of development, the proposed model produces either the in-phase or the antiphase mode of coordination by a simple change in the sign of the linear (visual) coupling between the two neuro-mechanical units. As such, the model is blind to any effect mentioned above with respect to the mode of coordination. To account for these features, future development of this model might include an error-correction mechanism (as mentioned previously) that would be based on the perceived relative phase. In a set of experiments, Bingham and colleagues investigated the visual perception of relative phase and revealed that relative phase variability was typically judged to be higher for the antiphase pattern than for the in-phase pattern (Bingham et al. 1999, 2001; Zaal et al. 2000). In a model for bimanual coordination, Bingham (2001, 2004) incorporated this experimental feature through a noise term with a variance that is a function of the difference in velocity between the movements of the two units. This difference being higher for the antiphase pattern, the model produced a higher variability in the latter condition. Assuming that an error mechanism would be less efficient for the antiphase case in which the perception of the relative phase is itself less adequate, the inclusion of such a mechanism in the model we propose has the potential to produce higher phase drift for the antiphase than for the in-phase pattern of coordination.

Acknowledgements This work was funded by the *UMR 6152* "Mouvement et Perception", CNRS-Université de la Méditerranée, Marseille, France. A. de Rugy is supported by a *University of Queensland Postdoctoral Research Fellowship* and O. Oullier was supported by the Programme Initiative-Postdoc of the *Fondation de l'Académie de Sciences.*

References

Amazeen PG, Schmidt RC, Turvey MT (1995) Frequency detuning of the phase entrainment dynamics of visually coupled rhythmic movements. Biol Cybern 72:511–518

Beek PJ, Peper CE, Daffertshofer A (2002) Modeling rhythmic interlimb coordination: beyond the Haken–Kelso–Bunz model. Brain Cogn 48:149–165

Bingham GP (1995) The role of perception in timing: feedback control in motor programming and task dynamics. In: Covey E, Hawkins H, McMullen T, Port R (eds) Neural representation of temporal patterns. Plenum, New York

Bingham GP (2001) A perceptually driven dynamical model of rhythmic limb movement and bimanual coordination. In: Proceedings of the 23rd annual conference of the cognitive science society. Lawrence Erlbaum Associates, Mahwah

Bingham GP (2004) A perceptually driven dynamical model of bimanual rhythmic movement (and phase perception). Ecol Psychol 16:45–53

Bingham GP, Schmidt RC, Turvey MT, Rosenblum LD (1991) Task dynamics and resource dynamics in the assembly of a coordinated rhythmic activity. J Exp Psychol Hum Percept Perform 17:359–381

Bingham GP, Schmidt, RC, Zaal FT (1999) Visual perception of the relative phasing of human limb movements. Percept Psychophys 61:246–258
Bingham GP, Zaal FT, Shull JA, Collins DR (2001) The effect of frequency on the visual perception of relative phase and phase variability of two oscillating objects. Exp Brain Res 136:543–552
Bressloff PC (1995) Average firing rate of a neural network with dynamical disorder. J Phys A Math Gen 28:2457–2469
Carson RG, Riek S, Bawa P (1999) Electromyographic activity, H-reflex modulation, and corticospinal input to forearm motoneurones during active and passive rhythmic movements. Hum Mov Sci 18:307–343
Carson RG, Riek S, Mackey DC, Meichenbaum DP, Willms K, Forner M, Byblow WD (2004) Excitability changes in human forearm corticospinal projections and spinal reflex pathways during rhythmic voluntary movement of the opposite limb. J Physiol 560:929–940
Cattaert D, Semjen A, Summers JJ (1999) Simulating a neural cross-talk model for between-hand interference during bimanual circle drawing. Biol Cybern 81:343–358
Challis J (1999) A procedure for the automatic determination of filter cut-off frequency for the processing of biomechanical data. J Appl Biomech 15:303–317
Collins DR, Sternad D, Turvey MT (1996) An experimental note on defining frequency competition in intersegmental coordination dynamics. J Mot Behav 28:299–303
Dempster W (1955) Space requirements of the seated operator. WADC Technical Report, 55–159, Report released to the Office of technical Services. U.S. Dept. Of Commerce, Washington
Fisher NI (1993) Statistical analysis of circular data. Cambridge University Press, Cambridge
Fitzhugh R (1957) Mathematical models of excitation and propagation in nerve. In: Schwan HP (ed) Biological engineering. McGraw-Hill, New York
Goldfield EC, Kay BA, Warren WH (1993) Infant bouncing: the assembly and tuning of action systems. Child Dev 64:1128–1142
Goodman L, Riley MA, Mitra S, Turvey MT (2000) Advantages of rhythmic movements at resonance: minimal active degrees of freedom, minimal noise, and maximal predictability. J Mot Behav 32:3–8
Hatsopoulos NG (1996) Coupling the neural and physical dynamics in rhythmic movements. Neural Comput 8:567–581
Hatsopoulos NG, Warren WH (1996) Resonance tuning in rhythmic arm movements. J Mot Behav 28:3–14
Jantzen KJ, Steinberg FL, Kelso JA (2004) Brain networks underlying human timing behavior are influenced by prior context. Proc Natl Acad Sci USA 101:6815–6820
Jirsa VK, Haken H (1997) A deviation of a macroscopic field theory of the brain from the quasi-microscopic neural dynamics. Physica D 99:503–526
Kelso J (1981) On the oscillatory basis of movement. Bull Psychon Soc 18:63
Kilner JM, Paulignan Y, Blakemore SJ (2003) An interference effect of observed biological movement on action. Curr Biol 13:522–525
Kugler PN, Turvey MT (1987) Information, natural law, and the self-assembly of rhythmic movement. Erlbaum, Hillsdale
Latash ML (1992) Virtual trajectories, joint stiffness, and changes in the limb natural frequency during single-joint oscillatory movements. Neuroscience 49:209–220
Liu Y-H, Wang X-J (2001) Spike-frequency adaptation of a generalized leaky integrate-and-fire model neuron. J Comput Neurosci 10:25–45
Nagumo J, Arimoto S, Yoshizawa S (1962) An active pulse transmission line simulating nerve axon. Proc Inst Radio Eng 50:2061–2070
Oullier O, de Guzman GC, Jantzen KJ, Kelso JAS (2003) On context dependence of behavioral variability in interpersonal coordination. Int J Comput Sci Sport 2:126–128
Peper CL, Beek PJ, Daffertshofer A (2000) Considerations regarding a comprehensive model of (poly)rhythmic movement. In: Desain P, Windsor L (eds) Rhythm perception and production. Swets and Zeitlinger, Lisse
Peper CE, Nooij SA, Van Soest AJ (2004a) Mass perturbation of a body segment: 2. Effects on interlimb coordination. J Mot Behav 36:425–441
Peper CL, Ridderikhoff A, Daffertshofer A, Beek PJ (2004b) Explanatory limitations of the HKB model: incentives for a two-tiered model of rhythmic interlimb coordination. Hum Mov Sci 23:673–697
de Rugy A, Sternad D (2003) Interaction between discrete and rhythmic movements: reaction time and phase of discrete movement initiation during oscillatory movements. Brain Res 994:160–174
de Rugy A, Wei K, Muller H, Sternad D (2003) Actively tracking 'passive' stability in a ball bouncing task. Brain Res 982:64–78
Russell DM, Sternad D (2001) Sinusoidal visuomotor tracking: intermittent servo-control or coupled oscillations? J Mot Behav 33:329–349
Schmidt RC, O'Brien B (1997) Evaluating the dynamics of unintended interpersonal coordination. Ecol Psychol 9:189–206
Schmidt RC, Turvey MT (1994) Phase-entrainment dynamics of visually coupled rhythmic movements. Biol Cybern 70:369–376
Schmidt RC, Carello C, Turvey MT (1990) Phase transitions and critical fluctuations in the visual coordination of rhythmic movements between people. J Exp Psychol Hum Percept Perform 16:227–247
Schmidt RC, Beek PJ, Treffner PJ, Turvey MT (1991) Dynamical substructure of coordinated rhythmic movements. J Exp Psychol Hum Percept Perform 17:635–651
Schmidt RC, Shaw BK, Turvey MT (1993) Coupling dynamics in interlimb coordination. J Exp Psychol Hum Percept Perform 19:397–415
Schmidt RC, Bienvenu M, Fitzpatrick PA, Amazeen PG (1998) A comparison of intra- and interpersonal interlimb coordination: coordination breakdowns and coupling strength. J Exp Psychol Hum Percept Perform 24:884–900
Sternad D, Turvey MT, Schmidt RC (1992) Average phase difference theory and 1:1 phase entrainment in interlimb coordination. Biol Cybern 67:223–231
Sternad D, Collins D, Turvey MT (1995) The detuning factor in the dynamics of interlimb rhythmic coordination. Biol Cybern 73:27–35
Sternad D, Amazeen EL, Turvey MT (1996) Diffusive, synaptic, and synergetic coupling: an evaluation through in-phase and anti-phase rhythmic movements. J Mot Behav 28:255–269
Sternad D, Saltzman EL, Turvey MT (1998) Interlimb coupling in a simple serial behavior: a task dynamic approach. Hum Mov Sci 17:393–433
Strogatz SH (1994) Nonlinear dynamics and chaos: with applications to physics, biology, chemistry, and engineering. Addison-Wesley, Reading
Taga G (1995a) A model of the neuro-musculo-skeletal system for human locomotion. I. Emergence of basic gait. Biol Cybern 73:97–111
Taga G (1995b) A model of the neuro-musculo-skeletal system for human locomotion. II Real-time adaptability under various constraints. Biol Cybern 73:113–121
Taga G (1998) A model of the neuro-musculo-skeletal system for anticipatory adjustment of human locomotion during obstacle avoidance. Biol Cybern 78:9–17
Temprado J-J, Laurent M (2004) Attentional load associated with performing and stabilizing a between-persons coordination of rhythmic limb movements. Acta Psychol (Amst) 115:1–16
Temprado J-J, Swinnen SP, Carson RG, Tourment A, Laurent M (2003) Interaction of directional, neuromuscular and egocentric constraints on the stability of preferred bimanual coordination patterns. Hum Mov Sci 22:339–363
Treffner P, Turvey MT (1995) Handedness and asymmetric dynamics of bimanual rhythmic coordination. J Exp Psychol Hum Percept Perform 21:318–333
Treffner PJ, Turvey MT (1996) Symmetry, broken symmetry, and handedness in bimanual coordination dynamics. Exp Brain Res 107:463–478
Turvey MT, Rosenblum LD, Schmidt RC, Kugler PN (1986) Fluctuations and phase symmetry in coordinated rhythmic movements. J Exp Psychol Hum Percept Perform 12:564–583
Van der Pol B (1926) On "relaxation oscillations". Phil Mag J Sci 2:978–992
Van Soest AJ, Peper CE, Selles RW (2004) Mass perturbation of a body segment: 1. Effects on segment dynamics. J Mot Behav 36: 419–424

Von Holst E (1973) Relative coordination as a phenomenon and as a method of analysis of central nervous system function. In: Marin R (ed) The behavioral physiology of animal and man. The collected papers of Erics Von Holst, vol 1. University of Miami Press, Coral Gables

Williamson MM (1998) Neural control of rhythmic arm movements. Neural Netw 11:1379–1394

Williamson MM (1999) Robot arm control exploiting natural dynamics. Unpublished PhD, MIT, Cambridge

Williamson MM (2003) Oscillators and crank turning: exploiting natural dynamics with a humanoid robot arm. Phil Trans A Math Phys Eng Sci 361:2207–2223

Wimmers RH, Beek PJ, van Wieringen PCW (1992) Phase transitions in rhythmic tracking movements: a case of unilateral coupling. Hum Mov Sci 11:217–220

Wing AM, Kristofferson AB (1973) Response delays and the timing of discrete motor responses. Percept Psychophys 14:5–12

Yamanishi J, Kawato M, Suzuki R (1980) Two coupled oscillators as a model for the coordinated finger tapping by both hands. Biol Cybern 37:219–225

Yu H, Russell DM, Sternad D (2003) Task-effector asymmetries in a rhythmic continuation task. J Exp Psychol Hum Percept Perform 29:616–630

Zaal FT, Bingham GP, Schmidt RC (2000) Visual perception of mean relative phase and phase variability. J Exp Psychol Hum Percept Perform 26:1209–1220